

# Scale dependent non- Gaussianity:

[as a way of explaining the existence of high redshift massive clusters]

Motivation and measurement.

**Ben Hoyle, Raul Jimenez, Licia Verde, ICC-IEEC University of  
Barcelona.**

**Geneva 12/3/2011**

# **Overview**

**Theoretical and observation motivation**

**Probes of non Gaussianity**

**More motivation!**

**The XMM Cluster Survey**

**Cluster of galaxies**

**Results (exciting, and not so exciting)**

**Future work**

# Motivation: theory, a window to the early Universe

Future planned experiments (e.g., gravitational wave or CMB polarization detectors) may be able to deduce the scale of inflation, by measuring either primordial gravitational waves directly or their effects on the polarization of the surface of last scattering.

But, using today's data, we can make a measurement of the primordial non-Gaussianity ( $f_{\text{NL}}$ ) which can tell us about the various types of scalar field interactions during inflation/reheating/preheating.

$$\Phi = \phi + f_{\text{NL}} (\phi^2 - \langle \phi^2 \rangle) .$$

## Generating scale independent non-Gaussianities:

Single field inflation: weak coupling during inflation typically result in a Gaussian field, but the decay of the field can be proportional to the square of the initial field, resulting in the primordial perturbations being non-Gaussian.  $f_{\text{NL}}$  here is usually scale dependent e.g., Byrnes et al 2010 [arXiv: 0911.2780]

## Generating scale dependent non-Gaussianities

One self coupled scalar field, can produce very small ( $<0.1$ ) scale dependent non-Gaussianities, or larger non-Gaussianities if they exhibit some non-linear evolution of modes after Hubble exit.

More than one (coupled self interacting) scalar field: in the early (preheating, reheating), or very early (inflation) Universe. e.g., Byrnes et al 2010 [arXiv: 1007.4277]

# Hand wavy theory for observers

Within the (perturbed) lagrangian for the scalar fields in the early universe

$$\Pi^2, (\partial\Pi)^2, \Pi_1\Pi_2 \rightarrow f_{NL} \lesssim 5 \neq f_{NL}(k)$$

**A single interacting field generates the power spectrum of the field with no (or v. small) deviations from Gaussianity.**

$$\Pi^3, (\partial\Pi)^3, \Pi(\partial\Pi)^2, \Pi_1\Pi_2\Pi_1 \rightarrow f_{NL}(k)(n_{NG}) \sim ?$$

**A single, multiply coupled field or two (or more) couple fields generate the bispectrum and can produce large non-Gaussianities (skewness) with scale dependence.**

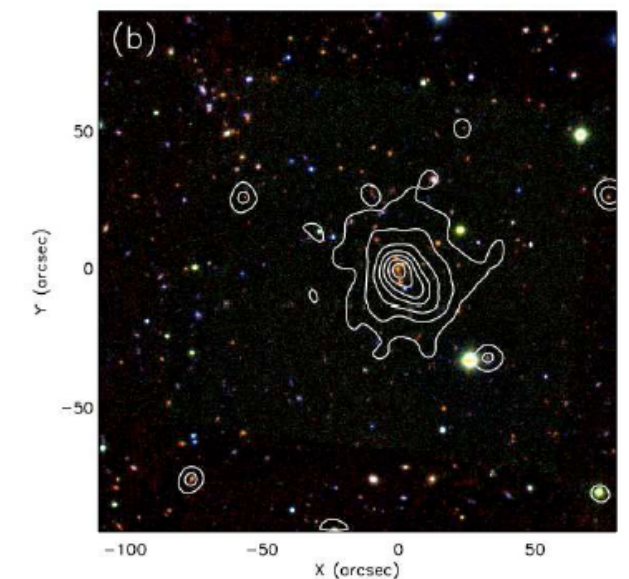
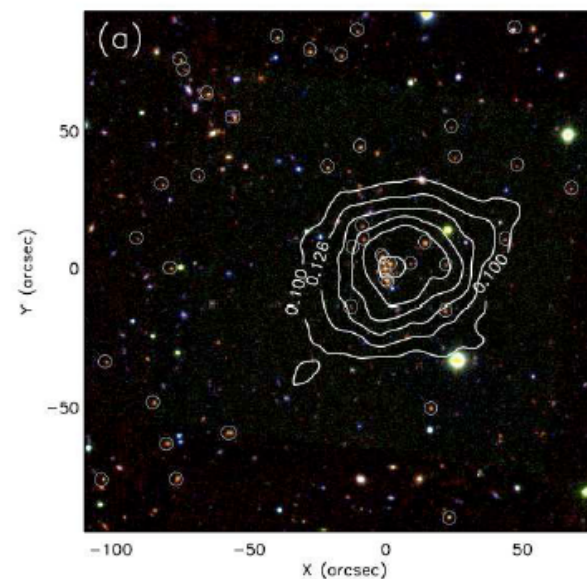
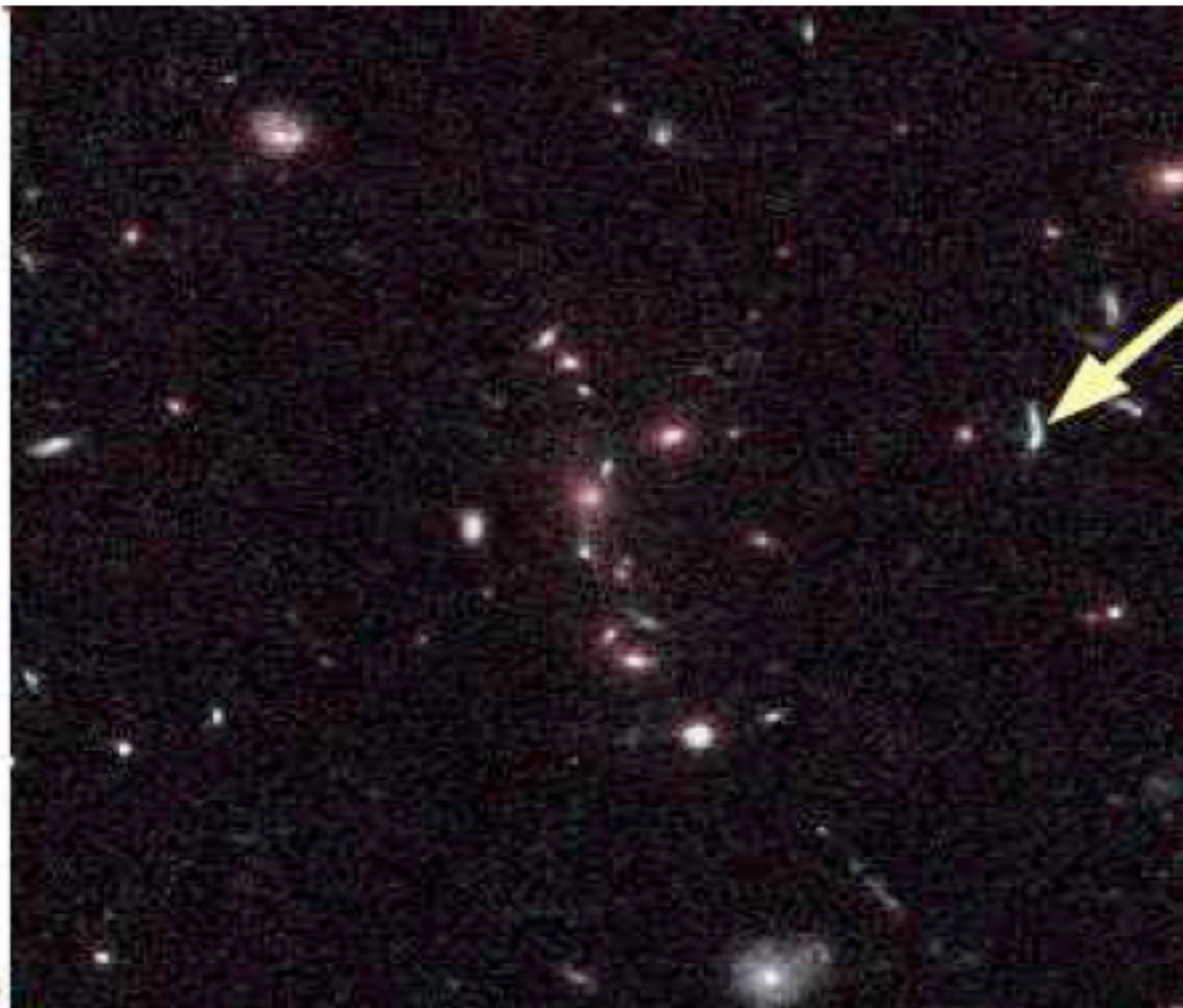
$$\Pi^4, \Pi_1^2\Pi_2^2, \Pi_1^2\Pi_2\Pi_3 \rightarrow f_{NL}, g_{NL}, \tau_{NL} \sim ?$$

**Many coupled /self interacting fields can produce trispectrum effects (kurtosis).**

# Motivation: observations

Some recent observations have called into question some of the underlying assumptions of the  $\Lambda$ CDM model + WMAP priors on the cosmological parameters. E.g., A very massive clusters of galaxies at high redshift, was statistically unlikely to have been observed.

## Galaxy cluster XMM J2235.



$$M_{200} = 7.7 \pm 1.3 \times 10^{14} M_{\odot}$$

$$M_{200} = 7.7^{+4.4}_{-3.3} \times 10^{14} M_{\odot}$$

$$z = 1.4$$

Jee et al 2009

**How likely was this cluster to be observed?**

**The expected number in the full sky  $\sim 7$ .**

**Footprint was 11 square degrees XMM X-ray survey, 0.02% of sky.**

**Poisson sample from  $(0.0002 \times 7) > 1$  only 1.4%**



# Improving our luck with non-Gaussianity

We can increase the number of expected clusters by allowing some  $f_{NL}$  which modifies the cluster mass function.

$$n_G(M, z) = \sqrt{\frac{2}{\pi}} \frac{\bar{\rho}}{M^2} \left| \frac{d}{d \ln M} \ln \sigma_M \right| \nu \exp -\nu^2/2. \quad \mathcal{R}_{NG}(S_{3,M}, M, z) = \frac{n(M, z, f_{NL})}{n_G(M, z, f_{NL} = 0)}$$

Solved in the Press-Schechter type formalism  
by Matarrese, Verde, Jimenez 2002,  
LoVerde et al 2007, D'Amico et al 2010

$$\mathcal{R}_{NG}(M, z, f_{NL}) = \exp \left[ \delta_{ec}^3 \frac{S_{3,M}}{6\sigma_M^2} \right] \times \left| \frac{1}{6} \frac{\delta_{ec}}{\sqrt{1 - \frac{\delta_{ec} S_{3,M}}{3}}} \frac{dS_{3,M}}{d \ln \sigma_M} + \sqrt{1 - \frac{\delta_{ec} S_{3,M}}{3}} \right|,$$

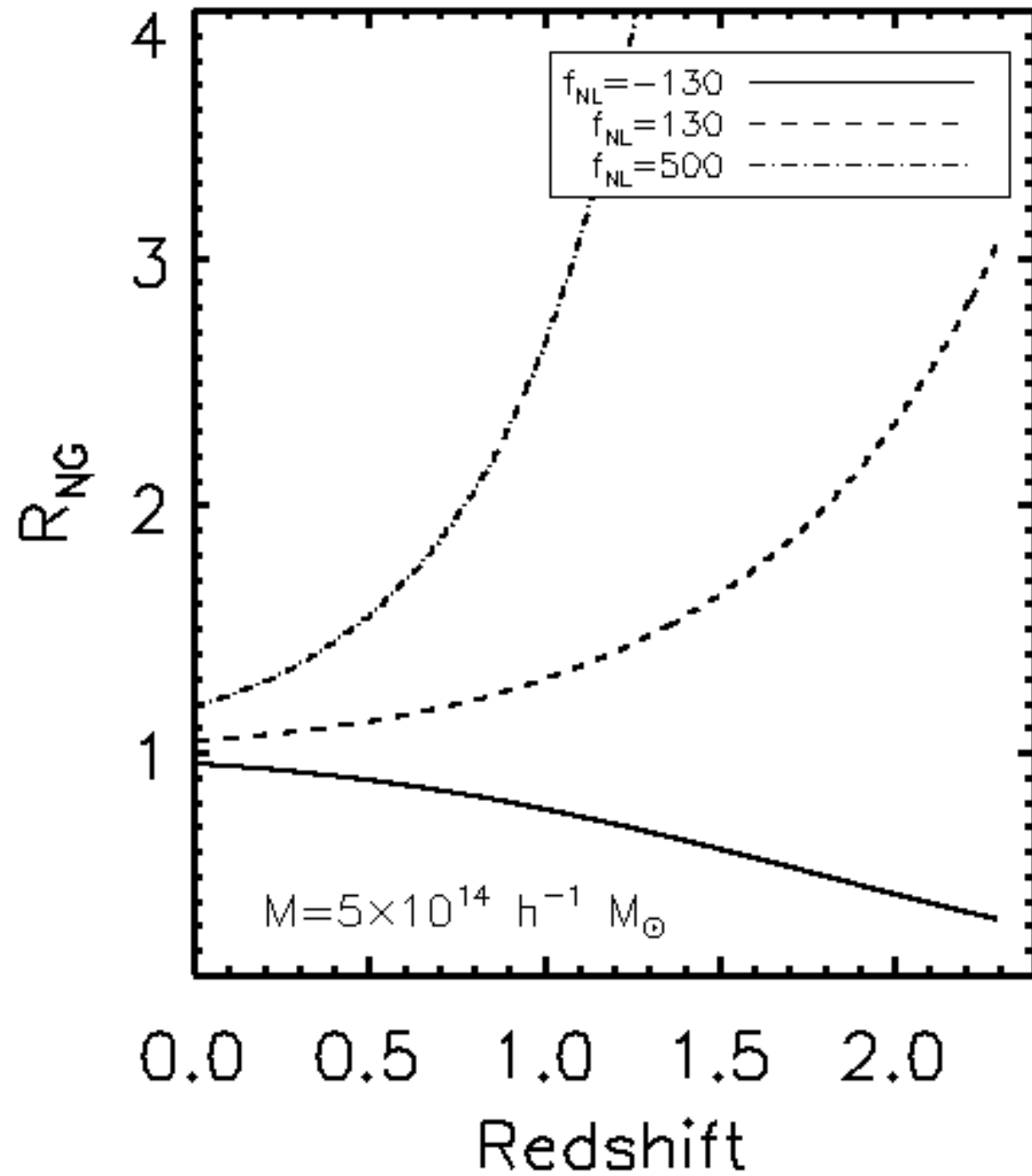
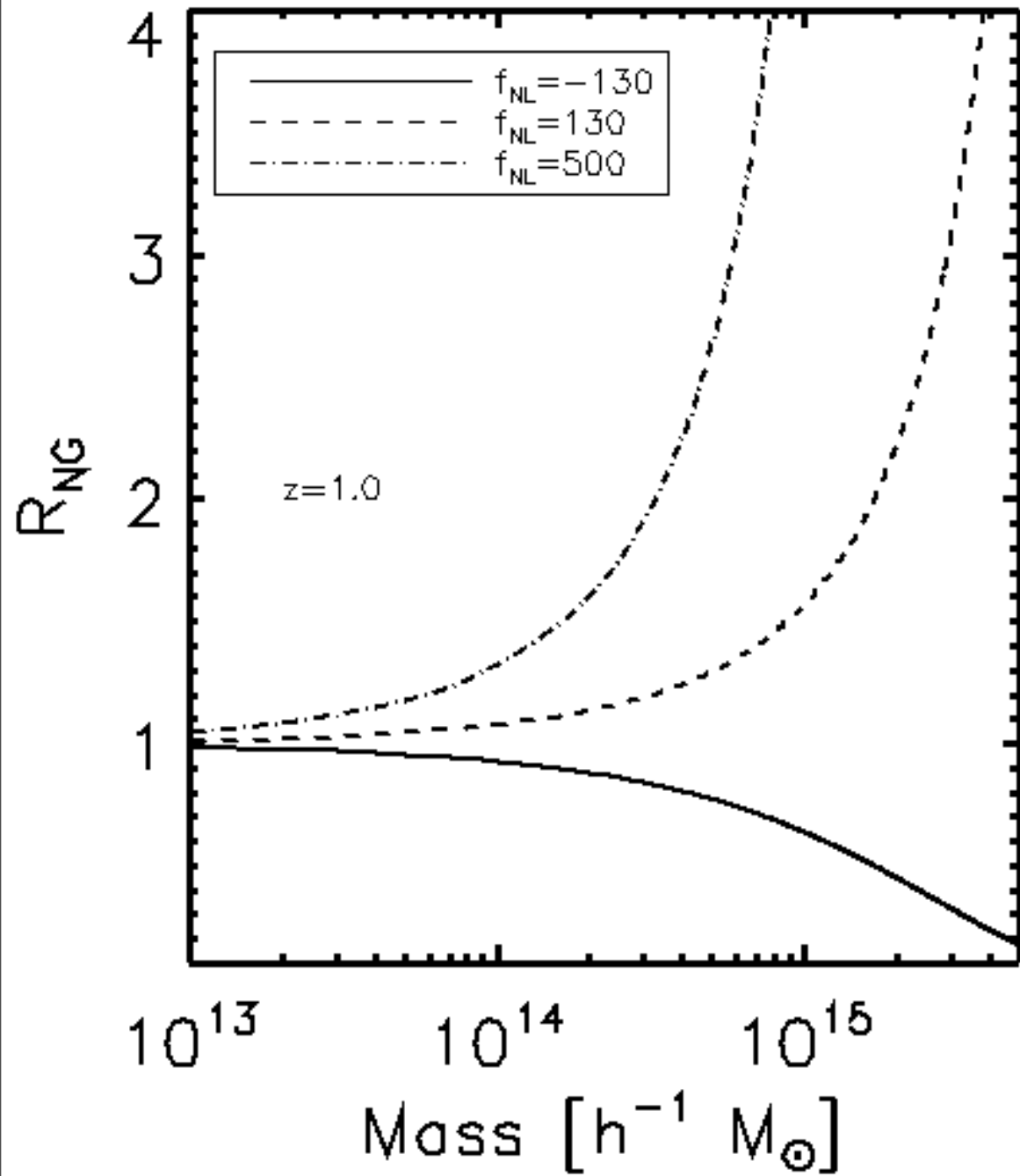
$S_{3,M}$  describes the normalised  
skewness of the smoothed density field

$$S_{3,M} = f_{NL} S_{3,M}^{f_{NL}=1}$$

Rng enable other, better calibrated mass functions to be used (Wagner et al 2010).

# Improving our luck

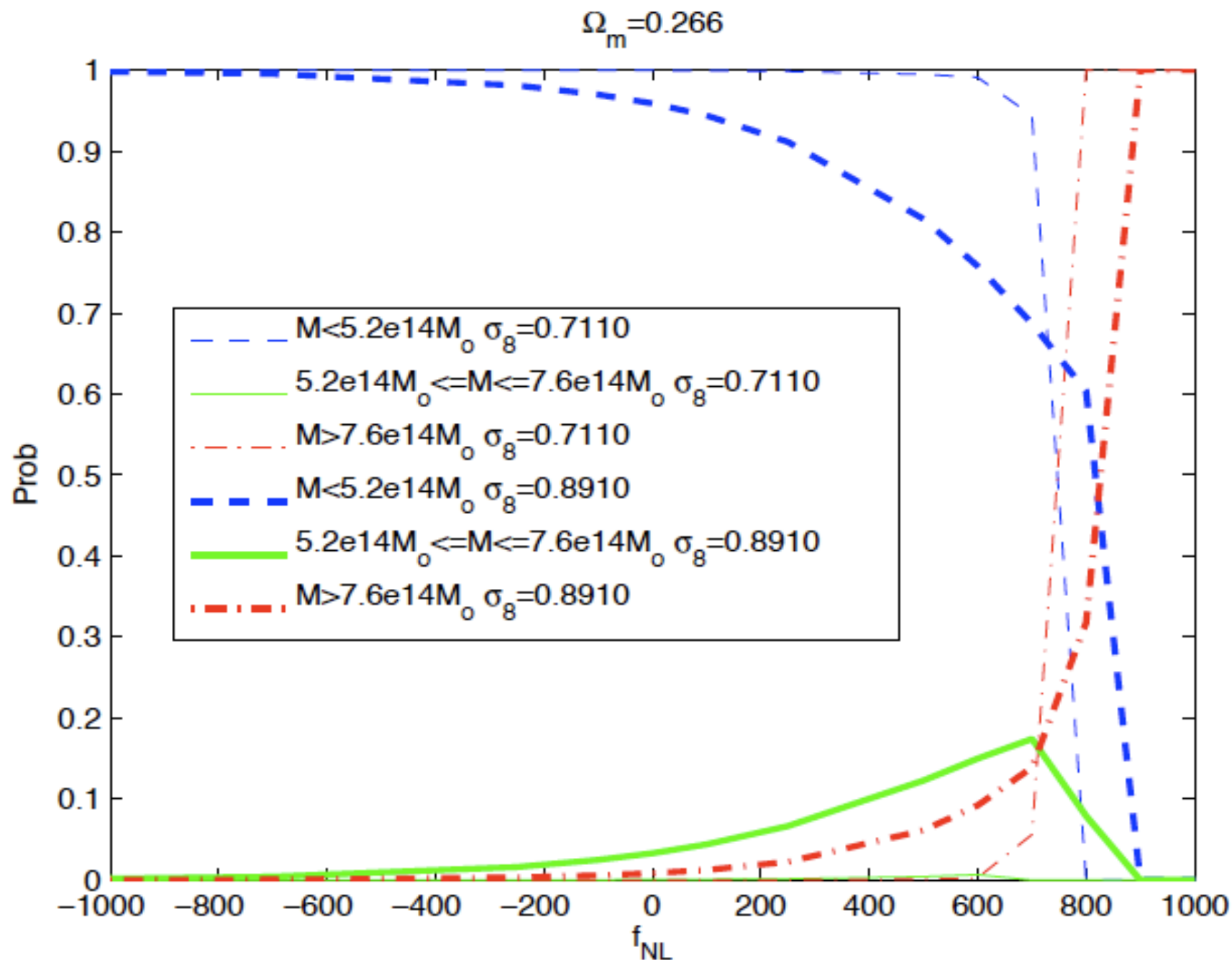
$$\mathcal{R}_{NG}(S_{3,M}, M, z) = \frac{n(M, z, f_{NL})}{n_G(M, z, f_{NL} = 0)}$$



**Jimenez & Verde 2009 showed values of  $f_{NL} \sim 150$  relieves tension with XMM J2235.**

# More work on XMM J2235

**Cayon et al 2010, calculated the probability that the “most massive” cluster in the survey footprint was a) more massive than the mass of the cluster, b) within the 1 sigma mass range of the cluster, c) less massive than the cluster**



**They modified the mass function with values of  $f_{NL}$ , and recalculated the probability.**

$$f_{NL} = 449 \pm 286 [1\sigma]$$

**Cayon et al 2010**



# Observations of non-Gaussianities at different scales

## The distribution of temperature anisotropies in the CMB

The bispectrum of the anisotropies and the correlation functions are related to  $f_{NL}$ . e.g., Yadav & Wandelt 2008, Komatsu et al 2011. Scales  $\sim 0.04$  h/Mpc

$$f_{NL} = \frac{\hat{S} - \hat{S}_{linear}}{N}$$

$S$  is an integral over the bispectrum (triangular shaped correlations),  $N$  related to the correlation matrix. Some hints of non Gaussianities have been seen.

$$27 < f_{NL} < 147, \text{ at the } 95\%$$

## The dark matter halo bias $b$ .

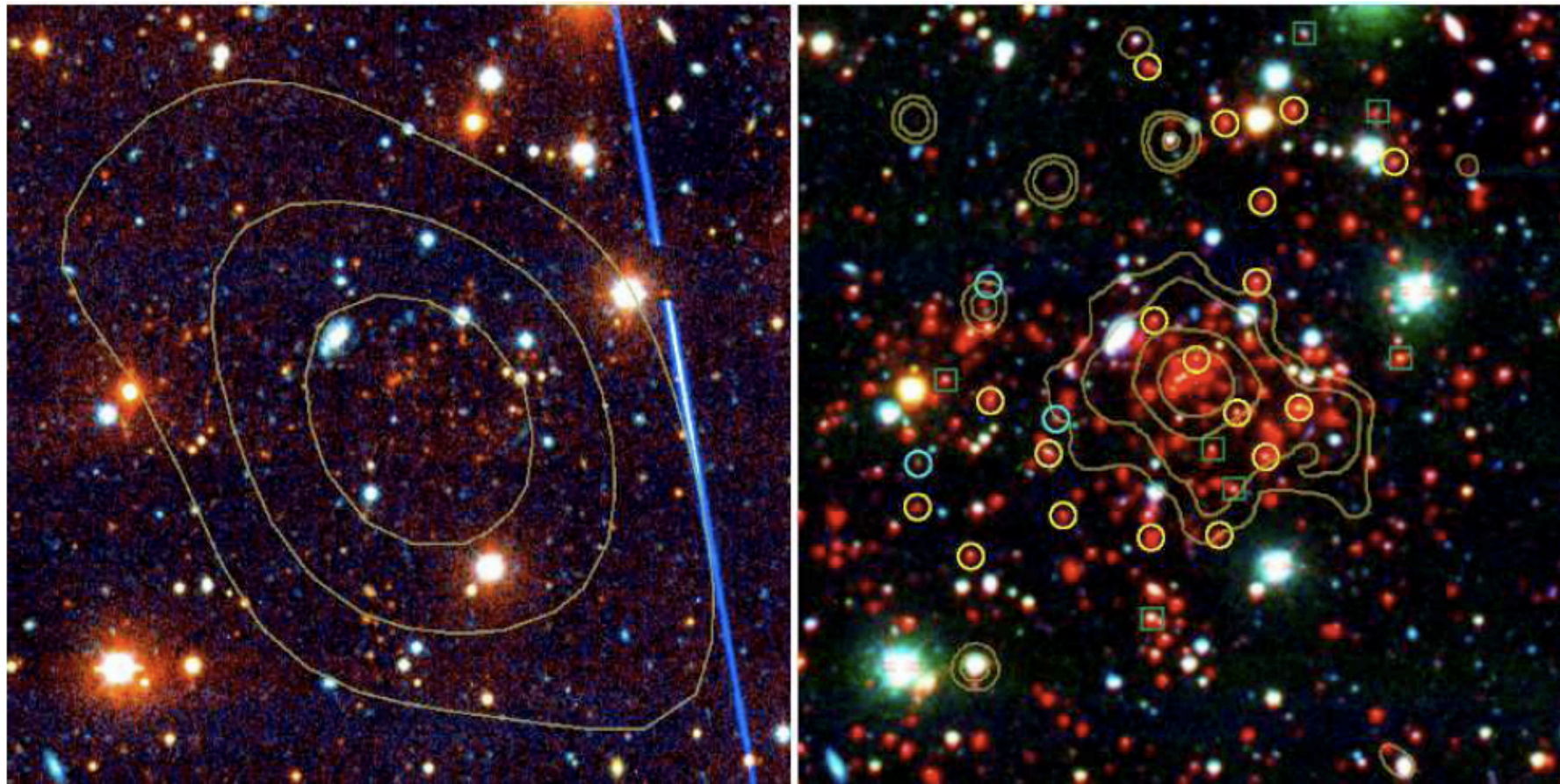
Signals of non Gaussianity from the bispectrum leak into the measurements of the two point correlation of dark matter halos. Galaxies sit at the peaks of the halos. e.g., Slozar et al 2008, Xia et al 2010. Scales  $\sim 0.1$  h/Mpc

$$\Delta b(M, k) = \frac{3\Omega_m H_0^2}{c^2 k^2 T(k) D(z)} f_{NL} \frac{\partial \ln n}{\partial \ln \sigma_8}$$

Where  $n$  is the local density, again some hints have been seen.

$$f_{NL} \sim 53 \pm 25 \text{ at } 1\sigma$$

# Motivation: observations II - another massive cluster



**SPT CL J0546-5345**

$$M_{200} = 1.27 \times 10^{15} M_{\odot}!$$

$$z = 1.05$$

**178 sq degrees  
survey footprint.**

**Expect 0.2  
clusters  
in this footprint**

**Poisson sample  
> 1 18%**

FIG. 1.— *Left:* Optical  $4' \times 4'$  color image (*grz*) of SPT-CL J0546-5345, with SZE significance contours overlaid ( $S/N = 2, 4,$  and  $6$ ). *Right:* False color optical (*ri*) + IRAC ( $3.6 \mu\text{m}$ ) image of SPT-CL J0546-5345, with *Chandra* X-ray contours overlaid ( $0.25, 0.4, 0.85$  and  $1.6$  counts per  $2'' \times 2''$  pixel per  $55.6$  ks in the  $0.5\text{-}2$  keV band). North is up, east is to the left. Due to its high angular resolution, *Chandra* is able to resolve substructure to the SW, which may be evidence of a possible merger. These images highlight the importance of IRAC imaging in studying the galaxies in high redshift, optically faint clusters. Spectroscopic early-type (late-type) members are indicated with yellow (cyan) circles. Green squares show the spectroscopic non-members.

**Brodwin et al  
2010**

Mass Type	Proxy	Measurement	Units	mass scaling Relation	$M_{200}^{a,b}$ ( $10^{14} M_{\odot}$ )
Dispersion	Biweight	$1179^{+232}_{-167}$	km/s	$\sigma$ - $M_{200}$ (Evrard et al. 2008)	$10.4^{+6.1}_{-4.4}$
	Gapper	$1170^{+240}_{-128}$	km/s	$\sigma$ - $M_{200}$ (Evrard et al. 2008)	$10.1^{+6.2}_{-3.3}$
	Std Deviation	$1138^{+205}_{-132}$	km/s	$\sigma$ - $M_{200}$ (Evrard et al. 2008)	$9.3^{+5.0}_{-3.2}$
X-ray	$Y_X$	$5.3 \pm 1.0$	$\times 10^{14} M_{\odot} \text{keV}$	$Y_X$ - $M_{500}$ (Vikhlinin et al. 2009)	$8.23 \pm 1.21$
	$T_X$	$7.5^{+1.7}_{-1.1}$	keV	$T_X$ - $M_{500}$ (Vikhlinin et al. 2009)	$8.11 \pm 1.89$
SZE	$Y_{SZ}$	$3.5 \pm 0.6$	$\times 10^{14} M_{\odot} \text{keV}$	$Y_{SZ}$ - $M_{500}$ (A10)	$7.19 \pm 1.51$
	S/N at 150 GHz	7.69		$\xi$ - $M_{500}$ (V10)	$5.03 \pm 1.13 \pm 0.77$
Richness	$N_{200}$	$80 \pm 31$	galaxies	$N_{200}$ - $M_{200}$ (H10)	$8.5 \pm 5.7 \pm 2.5$
	$N_{gal}$	$66 \pm 7$	galaxies	$N_{gal}$ - $M_{200}$ (H10)	$9.2 \pm 4.9 \pm 2.7$
Best	Combined				$7.95 \pm 0.92$

<sup>a</sup>  $M_{500}$  masses were scaled to  $M_{200}$  masses assuming an NFW density profile and the mass-concentration relation of Duffy et al. (2008).



# Motivation: observations III - yet another massive cluster!

SPT-CL J2106-5844,  $z=1.13$ , Survey footprint 2500 sq degrees.

Foley et al.

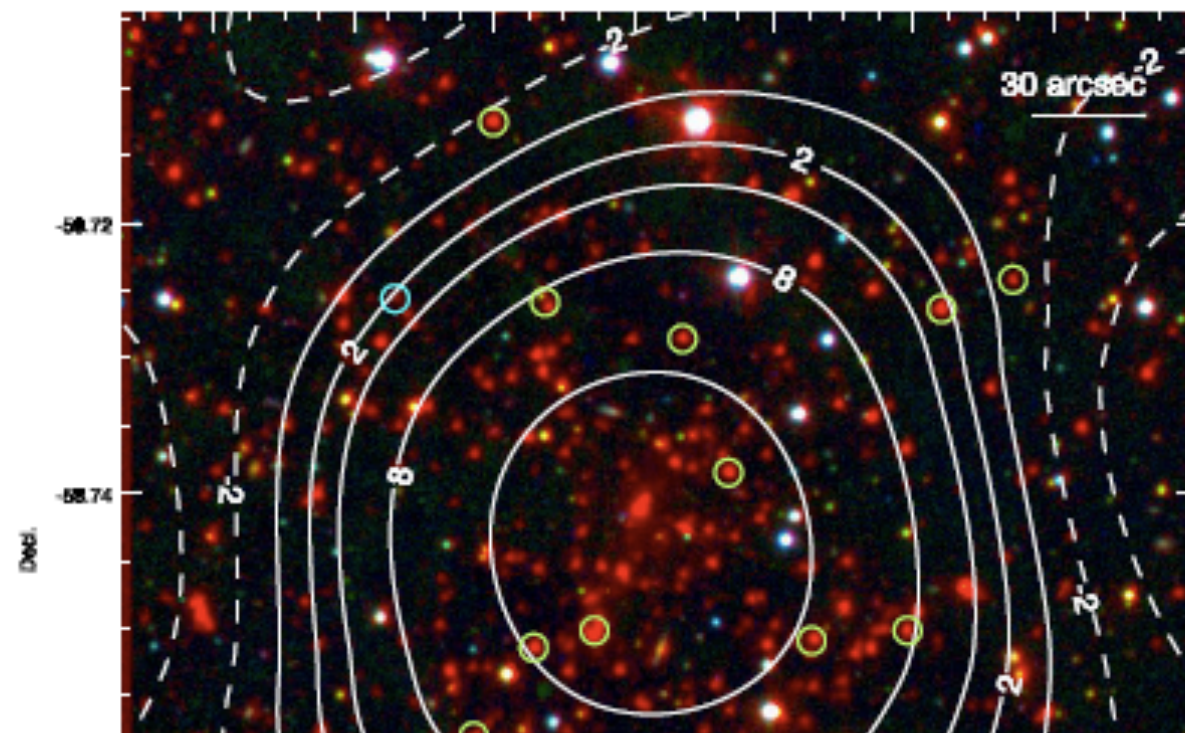
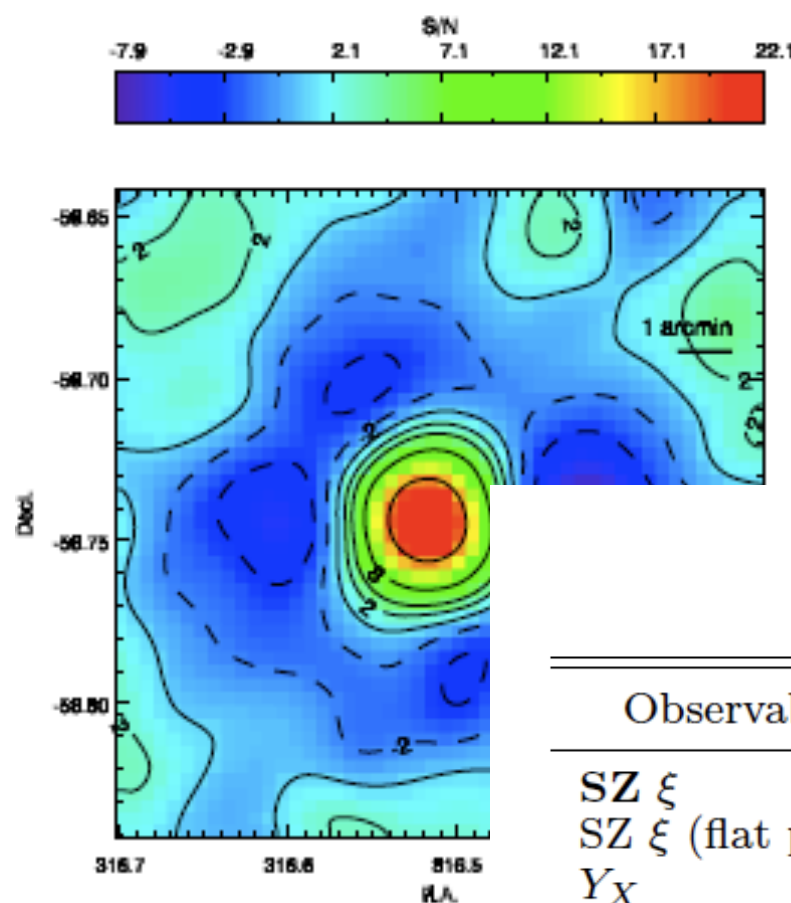


TABLE 2  
MASS ESTIMATES FOR SPT-CL J2106-5844

Observable	Measurement	$M_{200}(10^{15} h_{70}^{-1} M_{\odot})$
SZ $\xi$	18.5	$1.06 \pm 0.23$
SZ $\xi$ (flat prior)	18.5	$1.24 \pm 0.30$
$Y_X$	$(14.3 \pm 3.4) \times 10^{14} M_{\odot} \text{ keV}$	$1.85 \pm 0.40$
$T_X$	$11.0^{+2.6}_{-1.9} \text{ keV}$	$1.83 \pm 0.76$
$\sigma_v^a$	$1270^{+310}_{-220} \text{ km s}^{-1}$	$1.4^{+1.7}_{-0.8}$
Combined	...	$1.27 \pm 0.21$

Expect ONE cluster in the FULL sky, surveyed ~15% of the sky

# More clusters.

## What do multiple clusters tell us?

**Hoyle, Jimenez, Verde arXiv:1009.3884 [accepted PRD yesterday!], See also Enqvist, Hotchkiss, Taanila arXiv:1012.2732**

	Cluster Name	Redshift	$M_{200} \ 10^{14} M_{\odot}$	Method
	'WARPSJ1415.1+3612' +	1.02	$3.33^{+2.83}_{-1.80}$	Velocity dispersion
	'SPT-CLJ2341-5119' *	1.03	$7.60^{+3.94}_{-3.94}$	Richness
	'XLSSJ022403.9-041328' +	1.05	$1.66^{+1.15}_{-0.38}$	X-ray
<b><u>Data sample</u></b>	→'SPT-CLJ0546-5345' *	1.06	$10.0^{+6.00}_{-4.00}$	Velocity dispersion
	'SPT-CLJ2342-5411' *	1.08	$4.08^{+2.53}_{-2.53}$	Richness
<b>Spectroscopic redshifts</b>	'RDCSJ0910+5422' +	1.10	$6.28^{+3.70}_{-3.70}$	X-ray
	'RXJ1053.7+5735(West)' +	1.14	$2.00^{+1.00}_{-0.70}$	X-ray
<b>3 SZ detected</b>	'XLSSJ022303.0043622' +	1.22	$1.10^{+0.60}_{-0.40}$	X-ray
<b>   X-ray detected</b>	'RDCSJ1252.9-2927' +	1.23	$2.00^{+0.50}_{-0.50}$	X-ray
	'RXJ0849+4452' +	1.26	$3.70^{+1.90}_{-1.90}$	X-ray
	'RXJ0848+4453' +	1.27	$1.80^{+1.20}_{-1.20}$	X-ray
	→'XMMUJ2235.3+2557' +	1.39	$7.70^{+4.40}_{-3.10}$	X-ray
	'XMMXCSJ2215.9-1738' +	1.46	$4.10^{+3.40}_{-1.70}$	X-ray
	'SXDF-XCLJ0218-0510' +	1.62	$0.57^{+0.14}_{-0.14}$	X-ray

# XMM Cluster Survey

**Members: Kathy Romer [P.I], E. J. Lloyd-Davies, Mark Hosmer, Nicola Mehrrens, Michael Davidson, Kivanc Sabirli, Robert G. Mann, Matt Hilton, Andrew R. Liddle, Pedro T. P. Viana, Heather C. Campbell, Chris A. Collins, E. Naomi Dubois, Peter Freeman, Ben Hoyle, Scott T. Kay, Emma Kuwertz, Christopher J. Miller, Robert C. Nichol, Martin Sahlen, S. Adam Stanford, John P. Stott**

- **The XMM Cluster Survey aims to mine the XMM science archive for galaxy clusters**
- **The science goals of the XCS are:**
  - **To measure cosmological parameters  $\sigma_8$ ,  $\Omega_M$ ,  $\Omega_\Lambda$  to 5, 10 and 15 per cent accuracy respectively**
  - **To study the evolution of the cluster gas (i.e., the luminosity—temperature relation) to high redshift**
  - **To provide a sample of high redshift clusters that can be used to test theories of cluster galaxy formation and evolution**

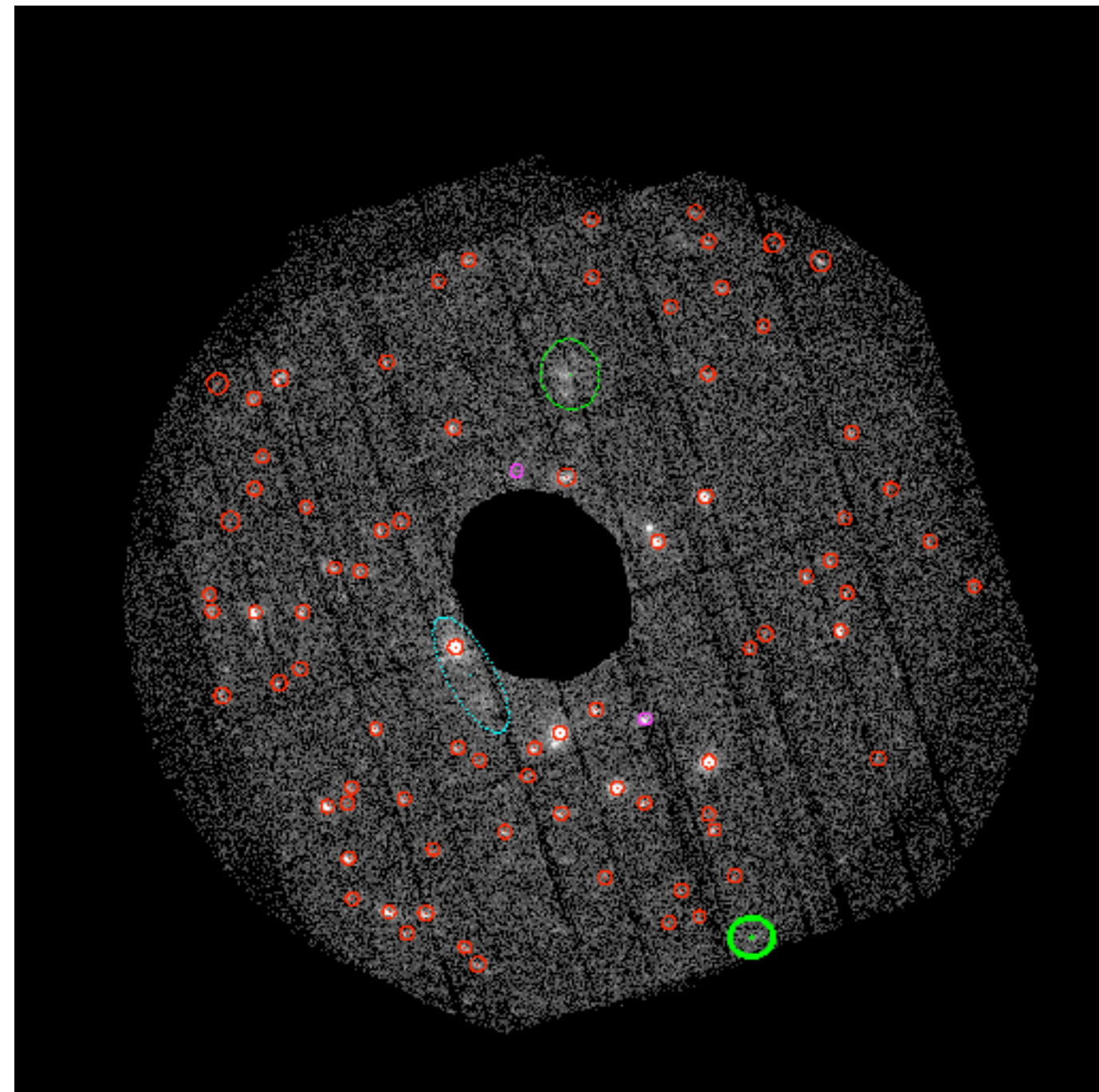


# Finding and classifying extended sources



**X-ray photon map + automated pipeline to detect point sources (red) and extended sources (green).**

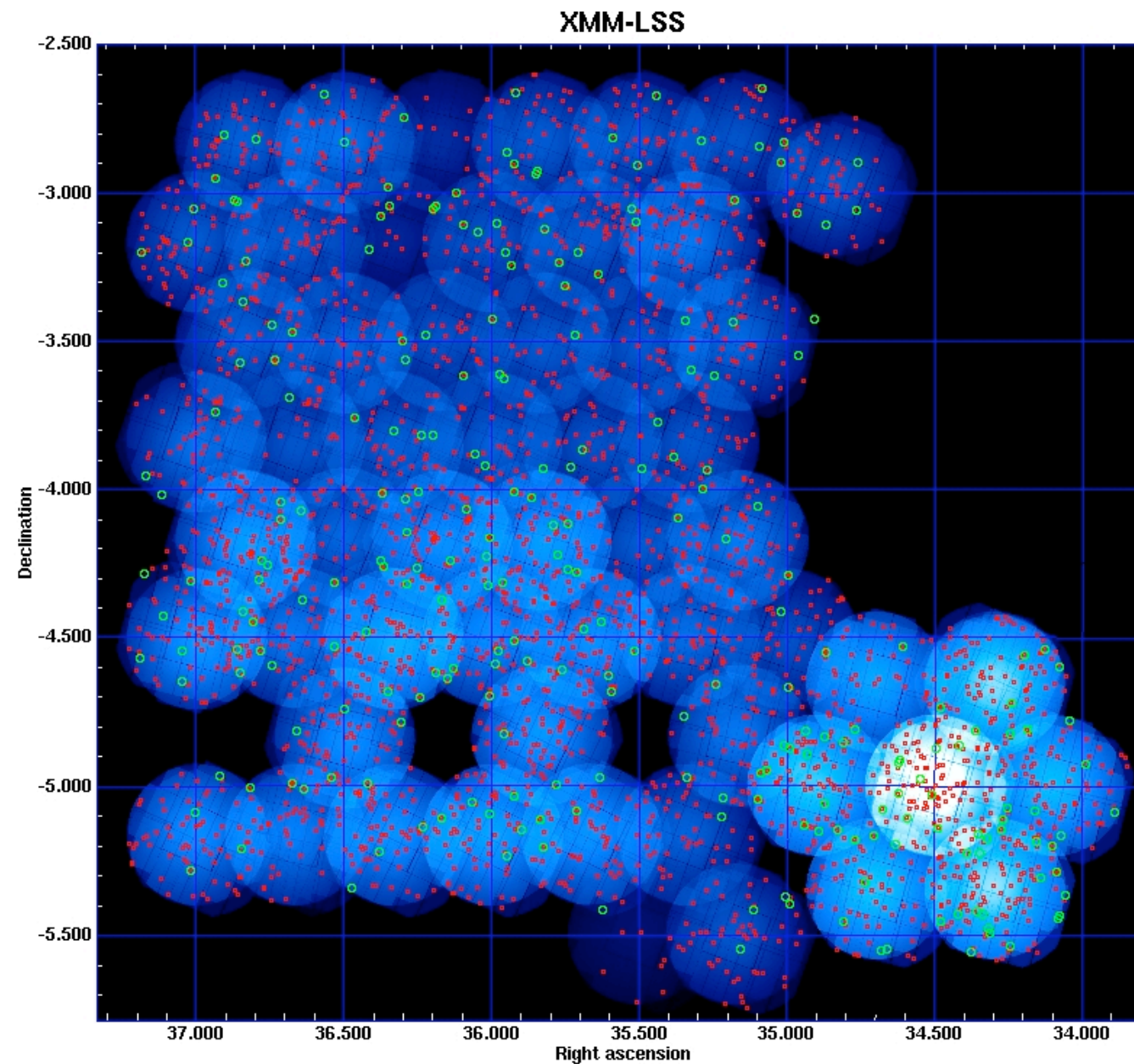
**X-ray emission is the smoking gun, but it's not enough. Need optical identification and redshifts (X-ray redshift difficult) before the fluxes can be converted to temperatures and masses.**





# An XCS Processed region

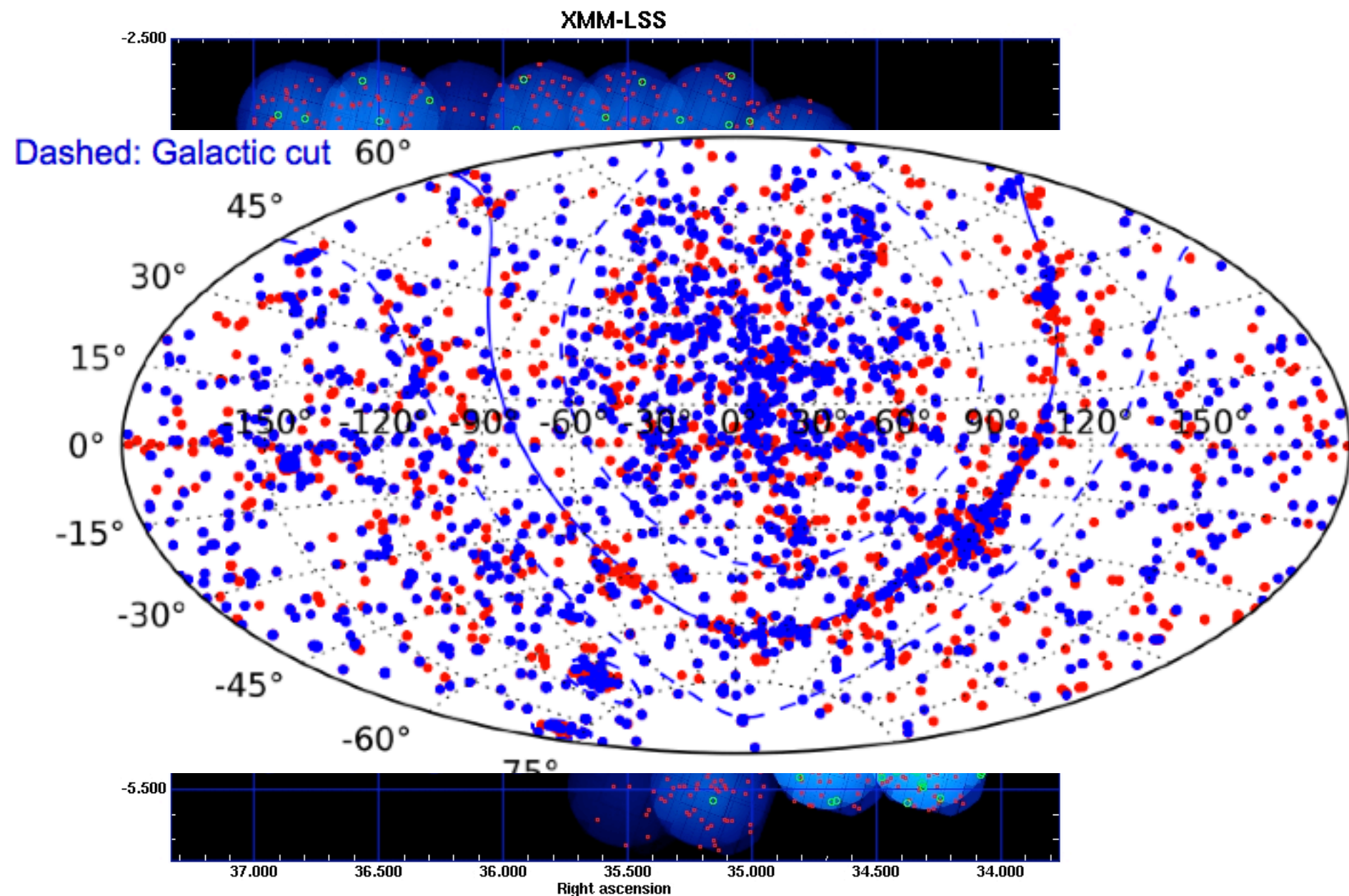
**To date, we have 500 sq. degrees processed - overlap corrected -  
and more than 4,000 cluster candidates catalogued**



- **Algorithms paper Lloyd-Davies et al. 2010 arXiv:1010.0677**

# An XCS Processed region

To date, we have 500 sq. degrees processed - overlap corrected -  
and more than 4,000 cluster candidates catalogued



- Algorithms paper Lloyd-Davies et al. 2010 arXiv:1010.0677

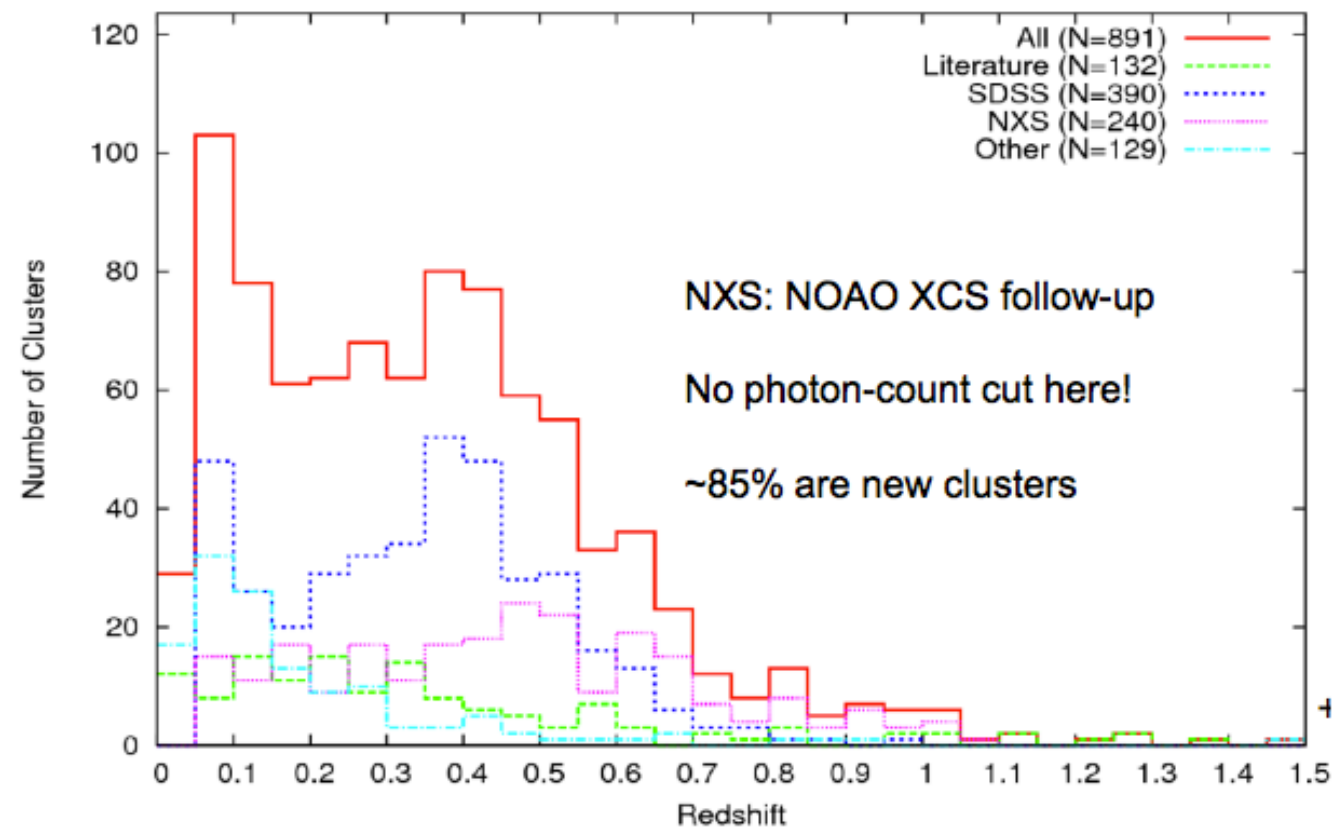


# Follow up strategy

- **XCS current status:**
  - **area = 500 deg<sup>2</sup>**
  - **candidates = 4000 (142 known previously)**
- **Imaging:**
  - **Archival: INT-WFS, EIS-XMM, SDSS**
  - **NOAO-XCS Survey (NXS): 330 CTIO pointings in r, z**
- **Redshift follow-up:**
  - **Low-z:**
    - photo-zs (NXS, SDSS)**
    - LRG z (SDSS)**
    - spectroscopy (NTT)**
  - **High-z:**
    - spectroscopy (Keck, Gemini, VLT)**





# Follow up strategy; Redshift distribution



**Mehrtens et al. in prep**

# Cluster Zoo

IUG, University of Portsmouth.

**XCS** extended source identification 

Hello Kath! Click here to [Log out](#)

### XCS classification page

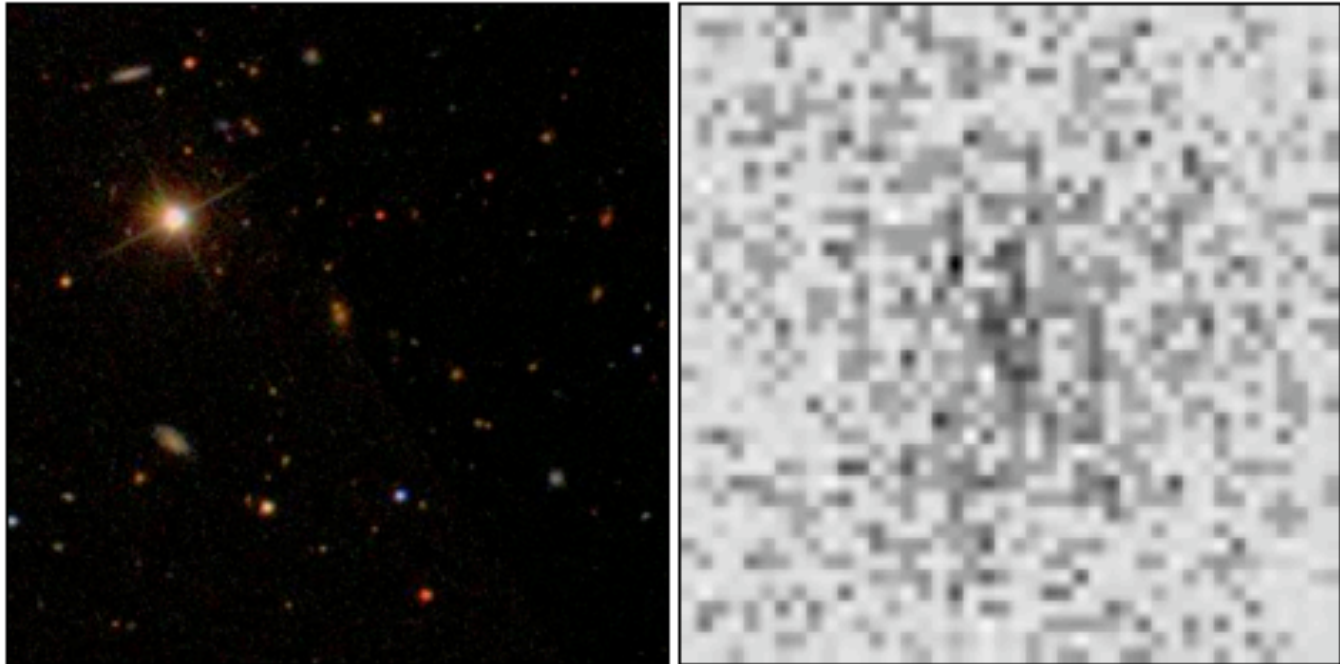
Please examine the figures found under the [Optical&X-ray images](#) and [Raw data](#) tabs, before making an extended source classification decision, under the third tab. This session you have made 0 classifications. Your target is 30. Access the [classifications here](#)

[Optical&X-ray images](#) [Mask data](#) [Make your classification](#)

### Optical and Xray images

Scrolling down the page displays images of the extended sources to be classified at three magnifications in the optical and x-ray. Simply moving [no need to click] your mouse over the contours: [\[on\]](#) and [\[off\]](#) links show and hide the contours, while [\[inv\]](#) inverts the sdss image, and highlights photometric objects. Don't like this cluster [Skip it here](#).

Magnification 3by3 sermins contours: [\[on\]](#) [\[inv\]](#) [\[off\]](#)



Magnification 4by4 sermins contours: [\[on\]](#) [\[inv\]](#) [\[off\]](#)


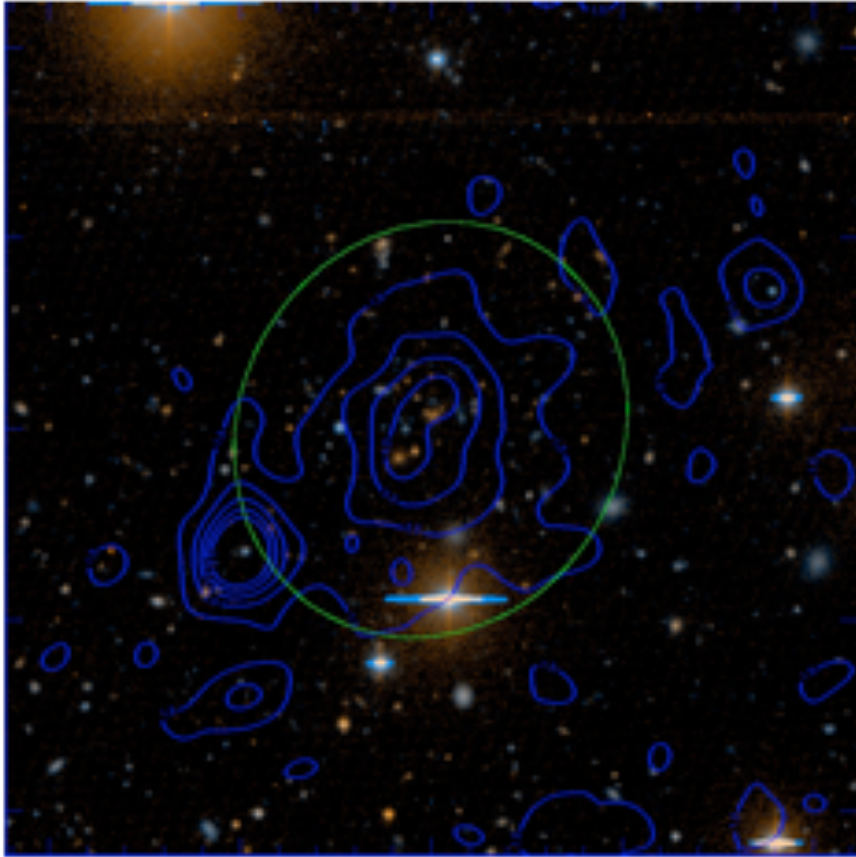
**Zoo created by B.H.**

# Cluster Zoo

IUG, University of Portsmouth.

Task 1: Please classify the cluster: XJ025006.4-310400.6

Photometric data	X-ray images
r-band: Seeing: 1.1401 Depth: 25.1828	3by3" : <input type="checkbox"/> no contours <input type="checkbox"/> contours
z-band: Seeing: 1.0231 Depth: 23.6477	6by6" : <input type="checkbox"/> no contours <input type="checkbox"/> contours
Image width (Arcmins): 2.24385	12by12" : <input type="checkbox"/> no contours <input type="checkbox"/> contours
X-ray Soft counts: 633.004	X-ray Soft counts: 633.004



Modification: (href="...")

**Zoo created by B.H.**



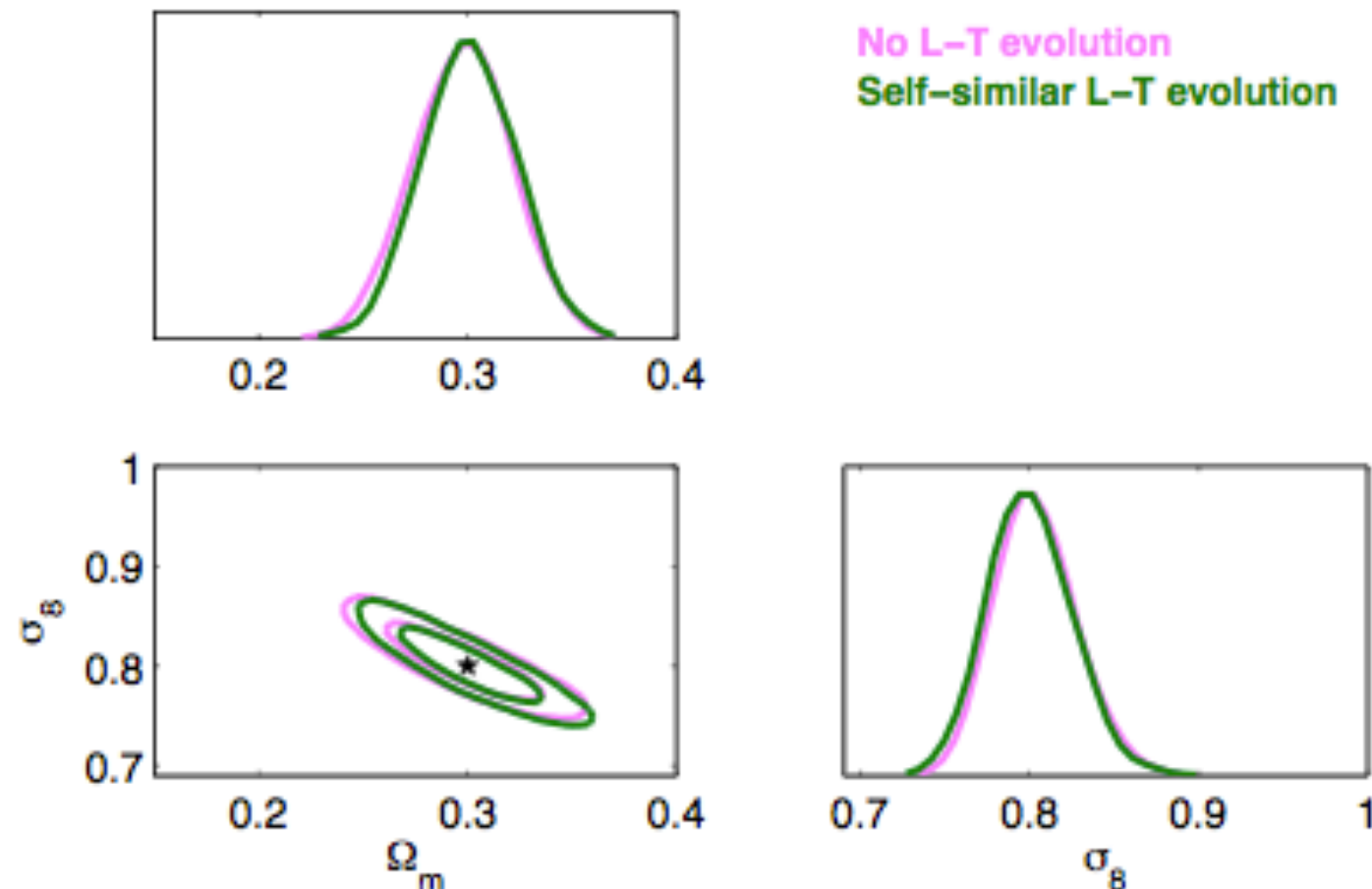
## Current X-Ray Cluster Surveys

Survey	Data	Clusters	Redshift range
HIFLUGCS	ROSAT	63	0.005 – 0.2
Maughan et al.	Chandra	115	0.1 – 1.3
O'Hara et al.	Chandra	70	0.18 – 1.24
400d	ROSAT/Chandra	86	0.35 – 0.9
XMM-LSS	XMM	29	0.05 – 1.05
Mantz et al.	ROSAT/Chandra	238	0.05 – 0.45
Peterson et al.	Chandra/XMM	723	0 – 1 ?
XCS <sub>300</sub> (230 $\square^\circ$ )	XMM	450	0.003 – 1.457

Martin Sahlen

**The next generation of Cluster samples will be found by X-ray  
(eRosita ~ 100,000) not SZ (ActPol ~ 1000)**

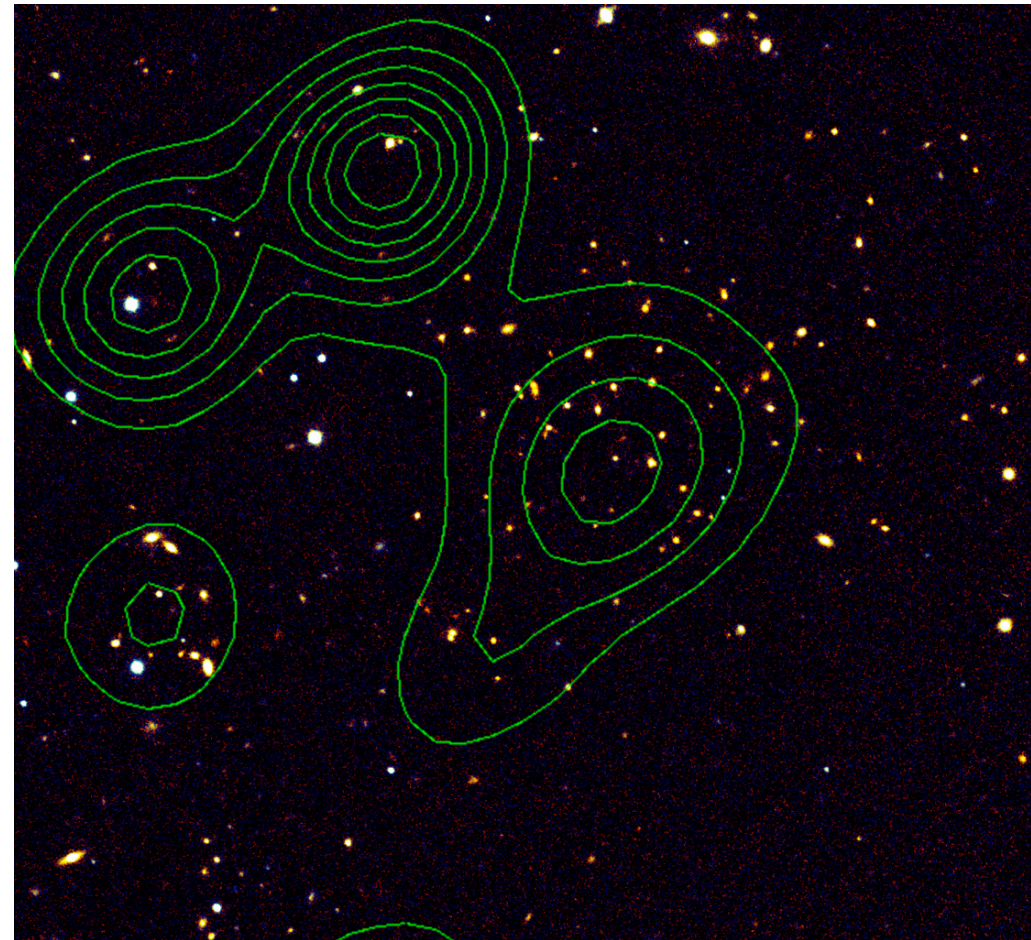
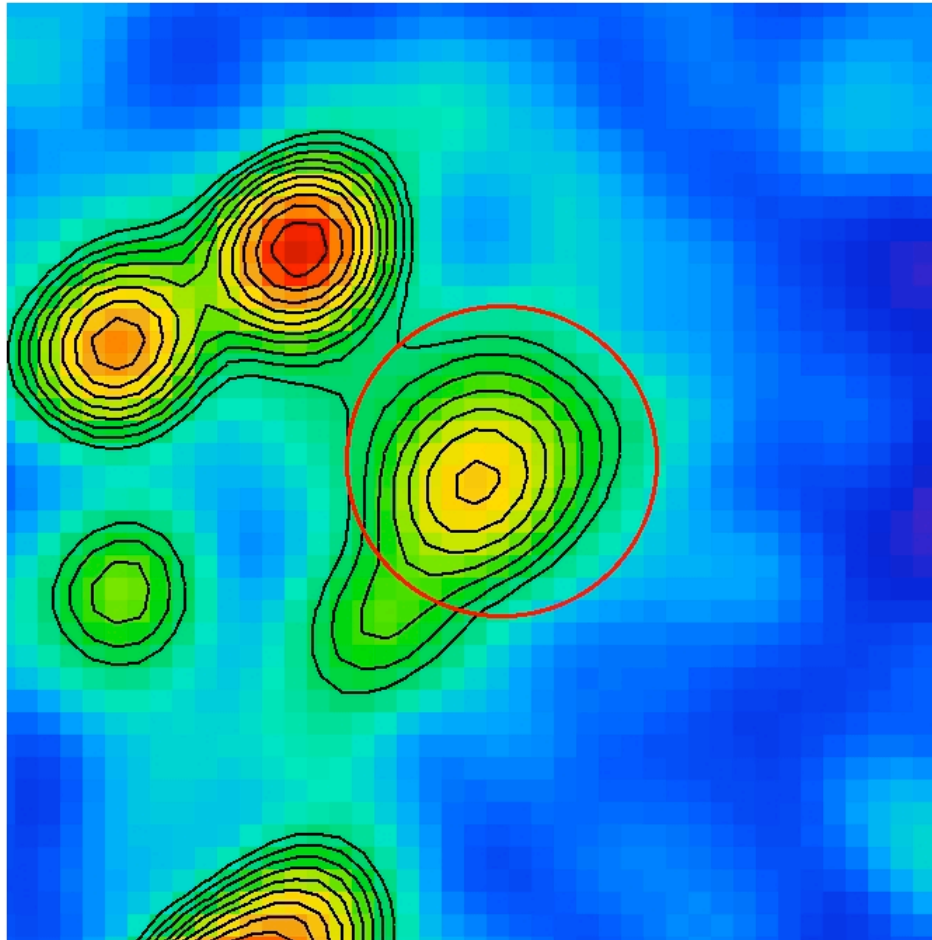
# XCS Cosmology predictions



- XCS predictions based on LCDM mock catalogue, XCS selection function (need to know LT relation), and MT relation
- Parameters derived from  $n(M,z)$  (Sahlen et al. 2009)

**Martin Sahlen**

# XMMXCS J2215.9-1738



**Was the highest redshift X-ray selected cluster,  $z=1.46$  (Stanford et al. 2006, Hilton et al. 2007, 2008)**

**Now  $z=2.07$ ,  $M \sim 5-8 \cdot 10^{13}$  SolMass, Gobat et al arXiv:1011.1837**



# More Clusters. Data sample

## Conservative assumptions

**Footprints; The clusters were found in the following surveys: XMM Cluster Survey, XMM Large Scale Survey, XMM Newton Distant Cluster Project, XMM Contiguous Survey, ROSAT deep survey, Wide Angle ROSAT Deep Survey.**

**There was overlap between the surveys. We conservatively assumed each X-ray survey had it's own unique footprint**

Cluster Name	Redshift	$M_{200} 10^{14} M_{\odot}$	Method
'WARPSJ1415.1+3612' +	1.02	$3.33^{+2.83}_{-1.80}$	Velocity dispersion
'SPT-CLJ2341-5119' *	1.03	$7.60^{+3.94}_{-3.94}$	Richness
'XLSSJ022403.9-041328' +	1.05	$1.66^{+1.15}_{-0.38}$	X-ray
→ 'SPT-CLJ0546-5345' *	1.06	$10.0^{+6.00}_{-4.00}$	Velocity dispersion
'SPT-CLJ2342-5411' *	1.08	$4.08^{+2.53}_{-2.53}$	Richness
'RDCSJ0910+5422' +	1.10	$6.28^{+3.70}_{-3.70}$	X-ray
'RXJ1053.7+5735(West)' +	1.14	$2.00^{+1.00}_{-0.70}$	X-ray
'XLSSJ022303.0043622' +	1.22	$1.10^{+0.60}_{-0.40}$	X-ray
'RDCSJ1252.9-2927' +	1.23	$2.00^{+0.50}_{-0.50}$	X-ray
'RXJ0849+4452' +	1.26	$3.70^{+1.90}_{-1.90}$	X-ray
'RXJ0848+4453' +	1.27	$1.80^{+1.20}_{-1.20}$	X-ray
→ 'XMMUJ2235.3+2557' +	1.39	$7.70^{+4.40}_{-3.10}$	X-ray
'XMMXCSJ2215.9-1738' +	1.46	$4.10^{+3.40}_{-1.70}$	X-ray
'SXDF-XCLJ0218-0510' +	1.62	$0.57^{+0.14}_{-0.14}$	X-ray

**Selection functions: For each cluster, we assumed that any similar (>M) cluster at any higher redshift would have been detected.**

**Survey volumes: We assumed all surveys had the redshift depth of the deepest survey  $z \sim 2.2$**

**Mass estimates: We chose to use the cluster mass and error which gave the least tension with LCDM**

# Analysis

**For each cluster “i”, we sample  $S$ , from the mass and error 10,000 times.  
We calculate the expected abundance of clusters above each sampled mass and redshift**

$$A_s = \int_{M_S}^{\infty} \int_{z=z_{cluster}}^{z=2.2} n(m, z, f_{NL}, C) dm dz$$

**Extending a Cayon et al approach, we Poisson sample  $P^O$ , from the expected abundance ( $A_s$ ) for this realisation.**

**If the Poisson sample is  $>1$ , the cluster exists in this realisation.**

**If the Poisson sample is  $<1$  the cluster does not exist in this realisation.**

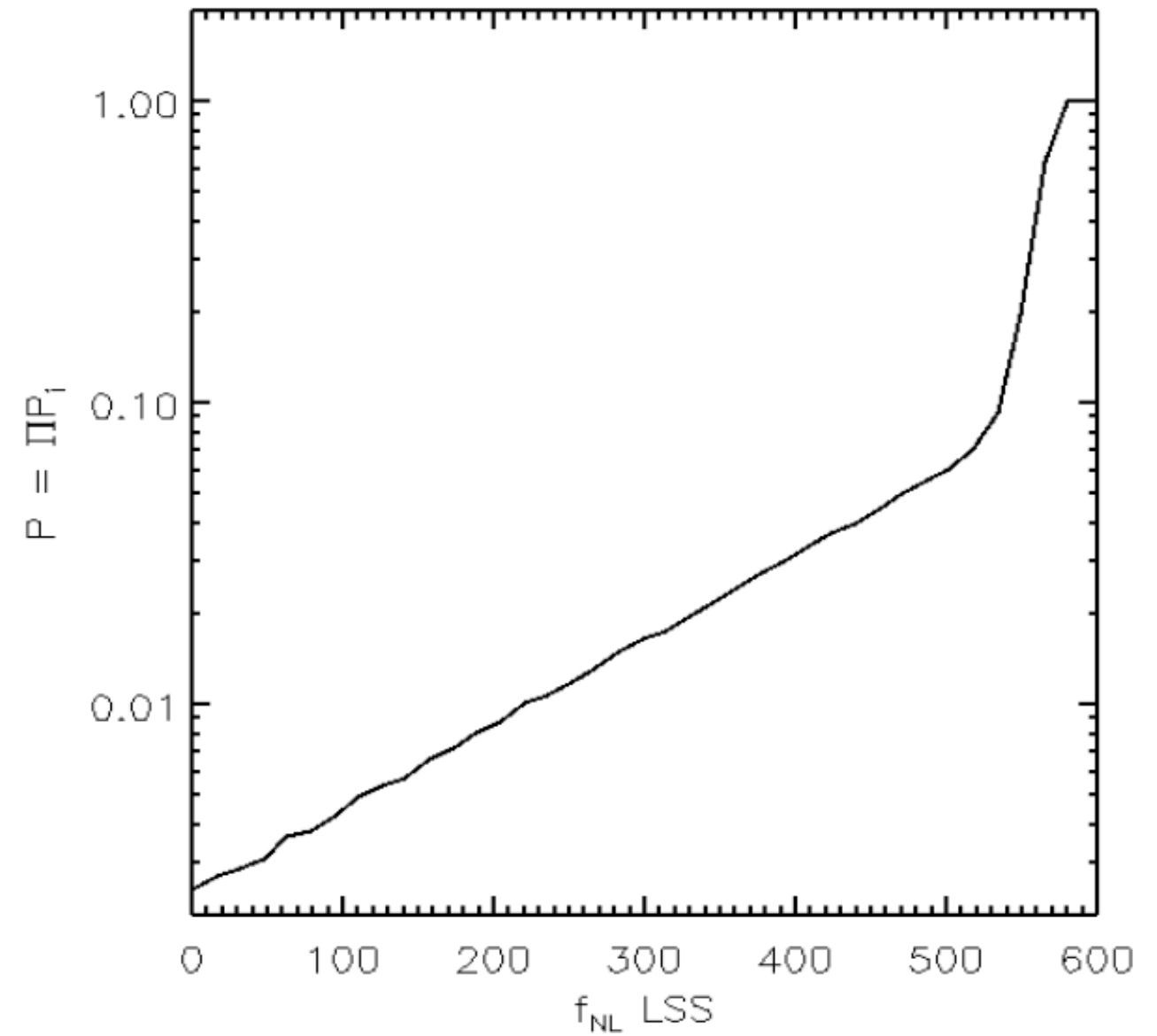
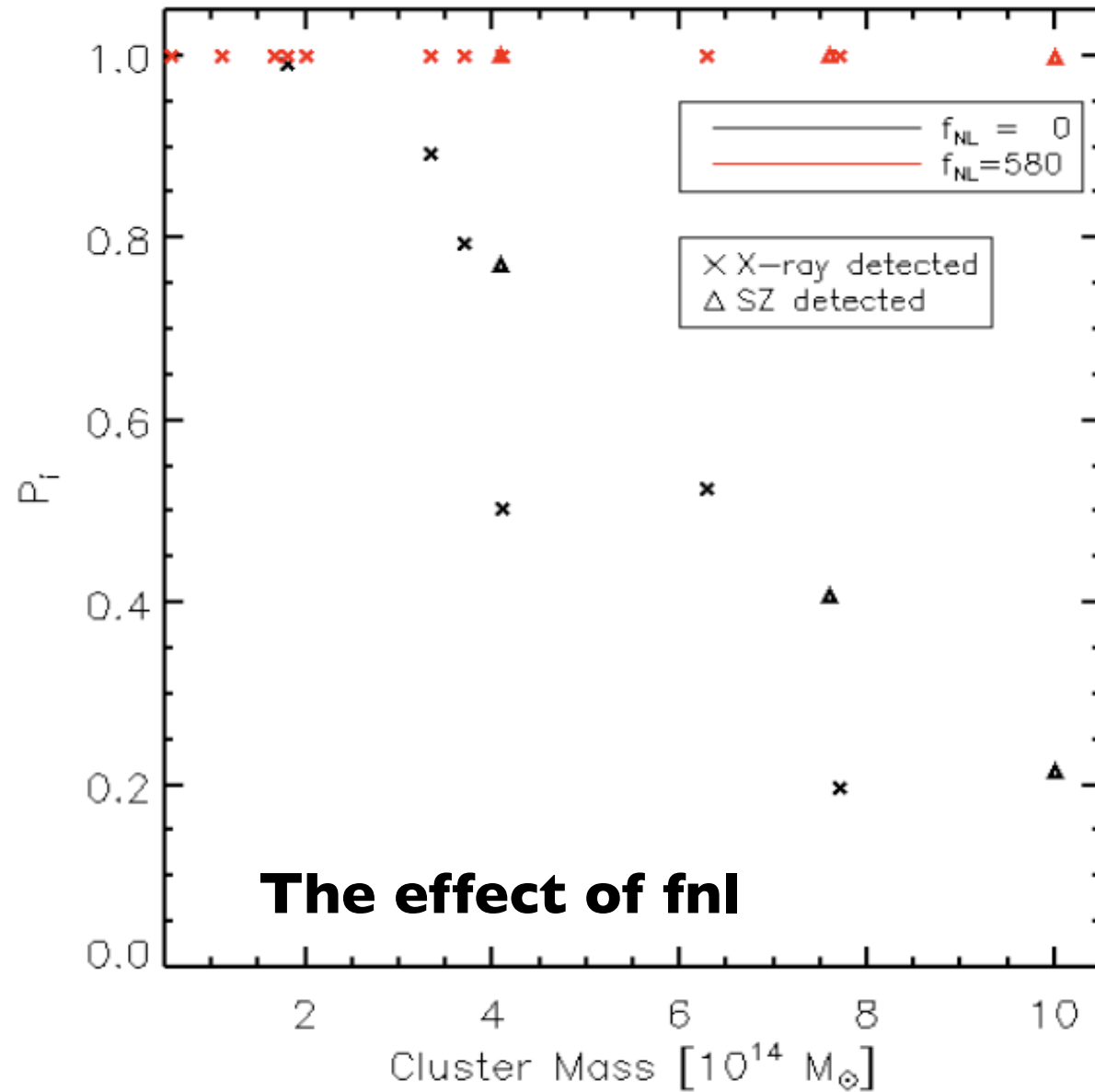
**The probability  $P_i$ , that cluster “i” exists is  $\text{Number}(P^O(A_s) \geq 1)/10^4$**

**The probability, that the ensemble of cluster exists is  $P(f_{NL}, C) = \prod P_i$**

**We multiply the probabilities, because the clusters are typically separated by vast redshifts, and positions on the sky. We therefore model them as being independent events.**

# Results I

Fixed cosmological parameters to best fit WMAP 5



**We determine the value of fnl where  $P=0.05$   
i.e., the value of fnl that contains 95% of the probability**

$$f_{NL} |_{P(0.05)}$$

At the 95% confidence level,  $f_{NL} > 467$

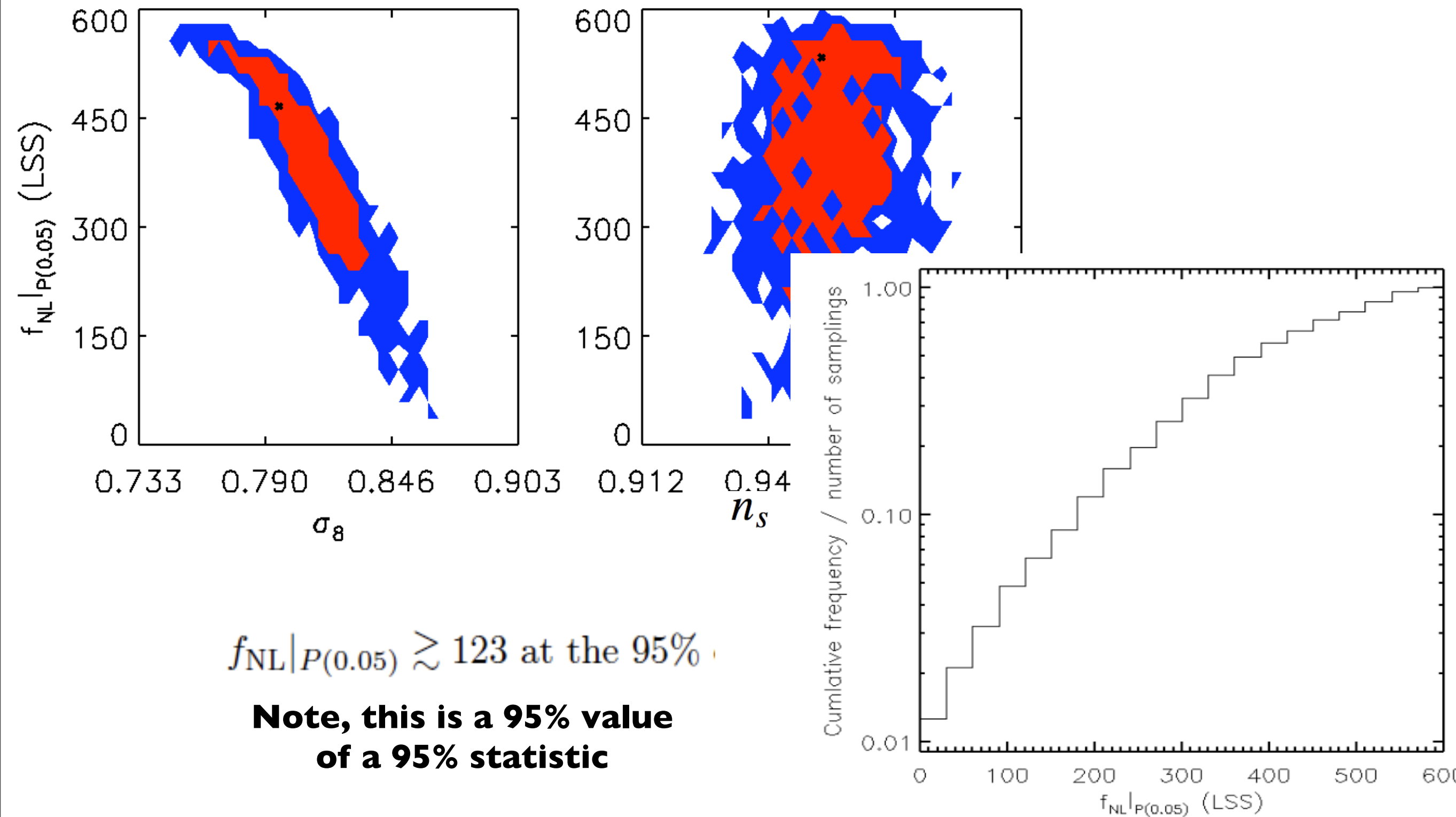
**Enqvist et al 2010  
arXiv:1012.2732**

$$f_{NL} \gtrsim 410$$



# Results II

Marginalising over parameters;  $\Omega_M, \Omega_b, \Omega_\Lambda, \Omega_K, n_s, \sigma_8, H_0, w_0$



$f_{NL|P(0.05)} \gtrsim 123$  at the 95%

**Note, this is a 95% value  
of a 95% statistic**

# Boring [-ish] Conclusions:

## Systematics.

**If every mass measurement was 1.5 sigma higher than the “true” value, then all tension is relieved. But all independent mass estimates must be equally wrong.**

## Cosmological parameters.

**If  $\sigma_8 \sim 0.9$ , but CMB + LSS finds**

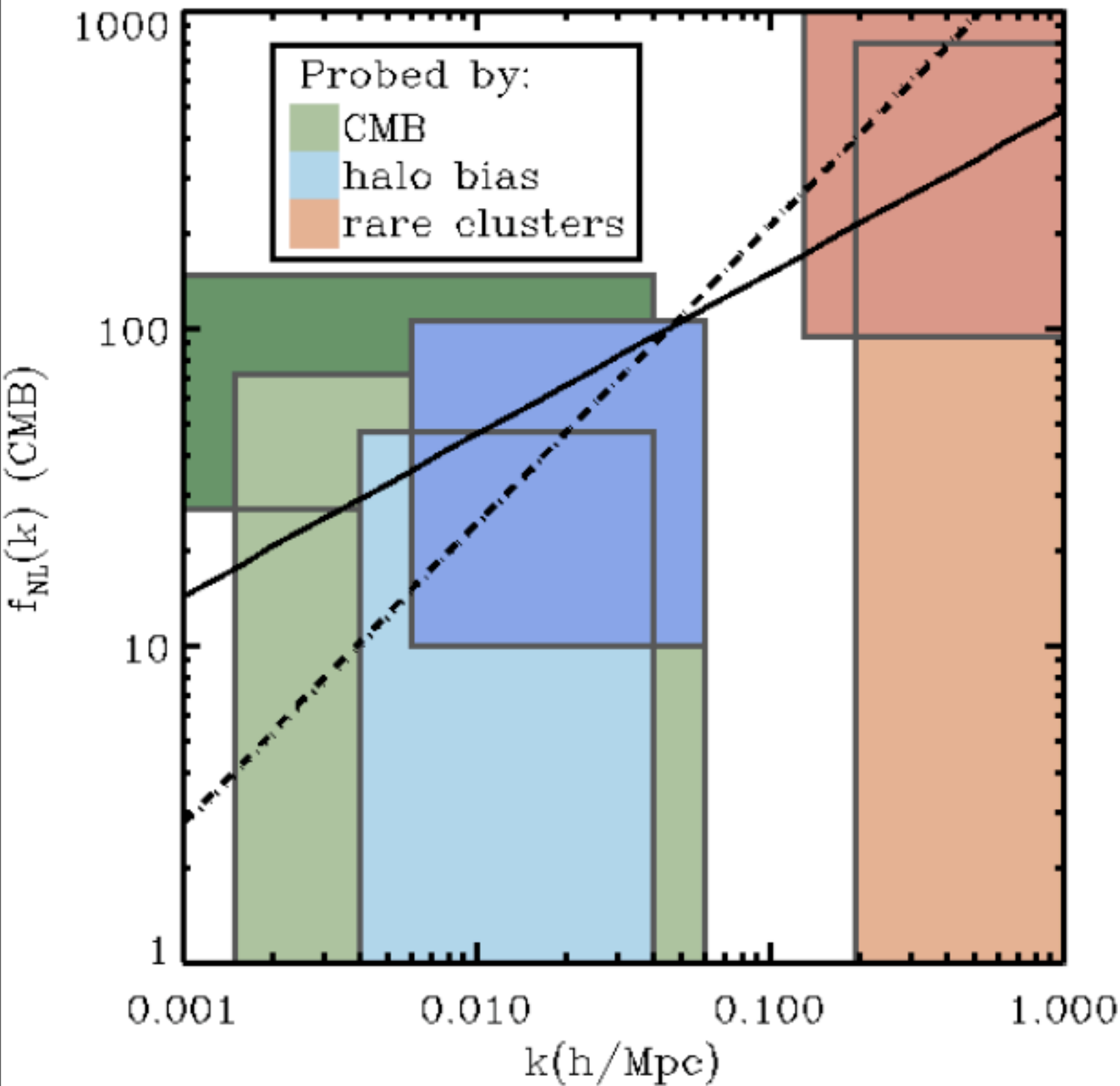
$$\sigma_8 = 0.801 \pm 0.03$$

**Komatsu et al 2011, so  $\sim 3$  sigma difference.**

## Mass functions.

**Do we understand the mass function with fnl at high mass and redshift well enough. On going work (Lo Verde & Smith last week)**

# Sexy Conclusions: Scale Dependent non-Gaussianity



**WMAP CMB, scales 0.04 h/Mpc**

$$27 < f_{NL} < 147, \text{ at the 95\%}$$

Yadev & Wandelt 2008

$$f_{NL} = 32 \pm 21 \text{ at } 1\sigma$$

Komatsu et al 2011

**Halo bias, scales 0.1 h/Mpc**

$$10 < f_{NL} < 106 \text{ at the 95\%}$$

Xia et al 2010

$$-77 < f_{NL} < 47 \text{ at the 95\%}$$

Slozar et al 2008

**Galaxy Clusters, scales 0.4 h/Mpc**

$$449 \pm 286 \text{ at } 1\sigma$$

Cayon et al 2010

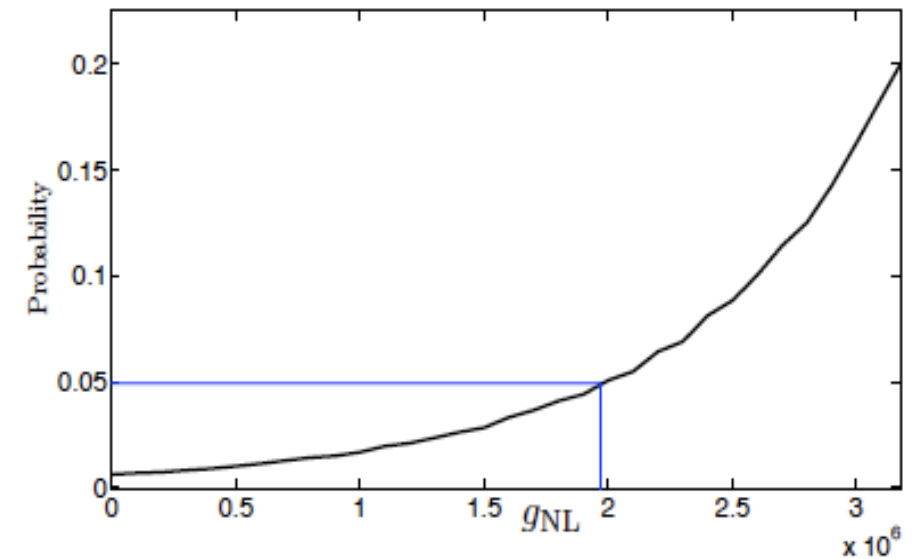
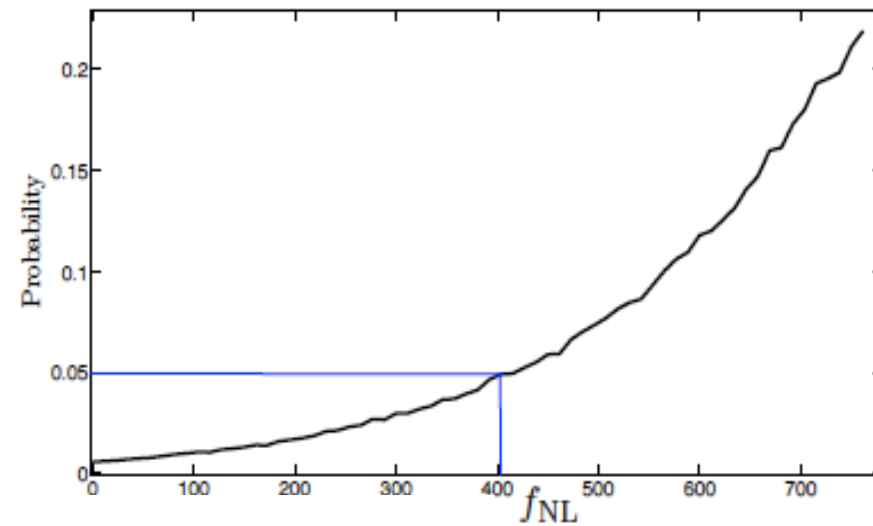
$$f_{NL|P(0.05)}^{LSS} \gtrsim 123 \text{ at the 95\%}$$

Hoyle et al 2010

$$f_{NL} = f_{NL}^* \left( \frac{k}{k^*} \right)^{n_{NG}} \quad n_{NG} = 0.50 \pm 0.19 \quad n_{NG} = 0.95 \pm 0.23$$

Lo Verde et al 2008

# Extensions/Related work



the ensemble of clusters in (b) The probability that the ensemble of clusters in the distribution of  $f_{NL}$ .

could exist as a function of  $g_{NL}$ , with  $f_{NL} \lesssim 50$ .

Figure 6. Estimates for  $f_{NL}$  and  $g_{NL}$ .

Enqvist et al 2010

**Showed how the choice of mass function leads to instability for large masses/values of  $f_{NL}$ , and extended for  $g_{NL}$ .**

$$\text{Let } f_{NL} < 50 \quad g_{NL} > 2.0 \times 10^6$$

Mortonson et al 2010 arXiv: 1011.0004

**Provided a fitting function to describe how one cluster could rule out LCDM.**

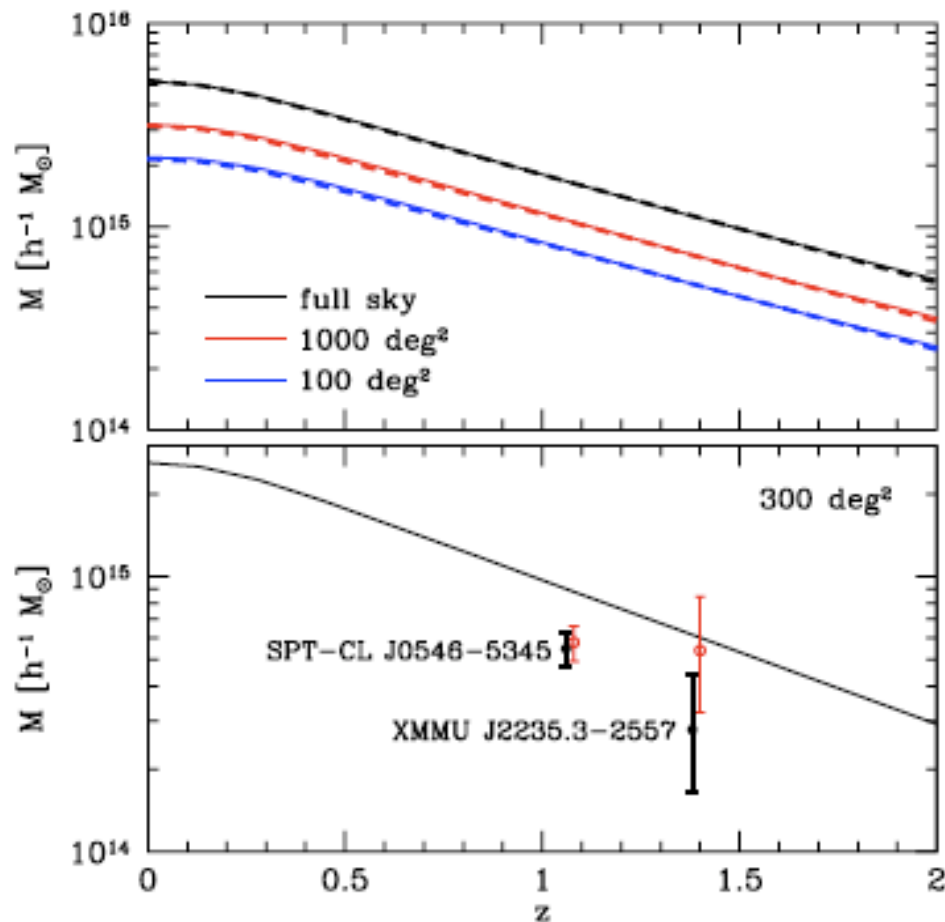


FIG. 4.  $M(z)$  exclusion curves. Even a single cluster with  $(M, z)$  lying above the relevant curve would rule out both  $\Lambda$ CDM and quintessence. Upper panel: flat  $\Lambda$ CDM 95% joint CL for both sample variance and parameter variance for various choices of sky fraction  $f_{sky}$  from the MCMC analysis (thin solid curves) and using

**Or, non constant equation of state of dark energy, Baldi & Pettorino 2010**

# Conclusions & future I

**These clusters pose a question to LCDM with WMAP priors on cosmological parameters.**

**Built a list of high redshift clusters.**

**Conservative assumptions.**

**Quantified the tension with LCDM.**

**Showed how  $f\sigma_8$  or systematics can reduce tension.**

**No consensus as to the level of tension, or how to quantify it.**

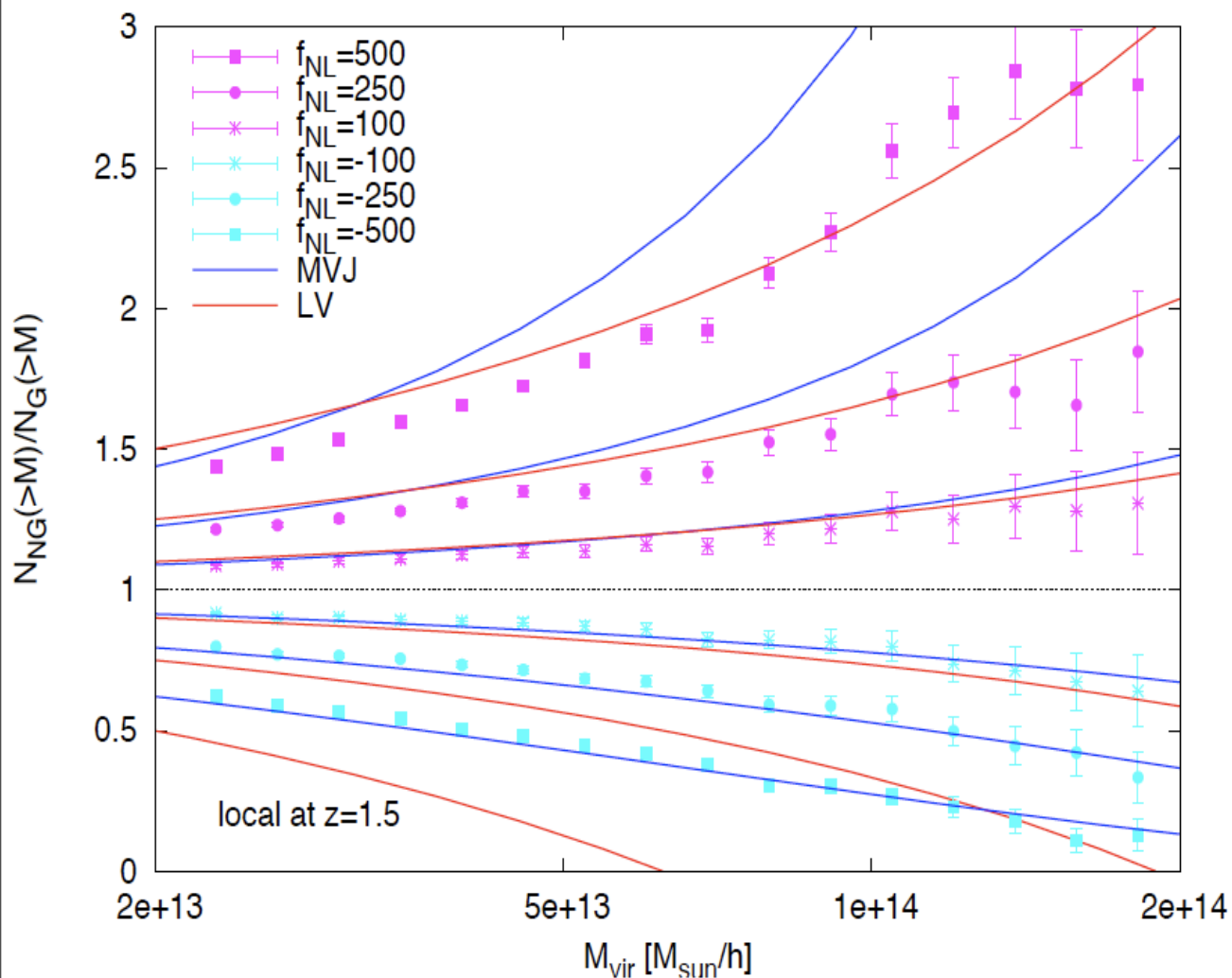
**But, more clusters are being found ~weekly. SPT release/Plank / X-ray, so we need a framework to understand what they tell us about LCDM**

# Conclusions & future II

**These clusters pose a question to LCDM with WMAP priors on cosmological parameters.**

**Theoretical/Computational:**

**Jorge Norena (Barcelona) is making available code to calculate the mass function with arbitrary  $f_{NL}$ ,  $g_{NL}$ ,  $t_{NL}$  (D'Amico et al 2010)**



**Non-Gaussian mass function fit to Nbody simulations (Christian Wagner et al 2010)**

**Mass function with  $f_{NL}, g_{NL}, t_{NL}$  Lo Verde & Smith arXiv:1102.1439**



# Conclusions & future III

These clusters pose a question to LCDM with WMAP priors on cosmological parameters.

**Better mass estimates for a sample of high redshift clusters, with an HST proposal [Ben Hoyle [P.I.], Aday Robiana, Licia Verde, Raul Jimenez, David Bacon, Martin Sahlen, Ed Lloyed-Davies, Kathy Romer, Matt Hilton, Nicola Mehrrens.]**

